Behavioral/Systems/Cognitive

Adaptation of Velocity Encoding in Synaptically Coupled Neurons in the Fly Visual System

Julia Kalb, Martin Egelhaaf, and Rafael Kurtz
Department of Neurobiology, Bielefeld University, D-33501 Bielefeld, Germany

Although many adaptation-induced effects on neuronal response properties have been described, it is often unknown at what processing stages in the nervous system they are generated. We focused on fly visual motion-sensitive neurons to identify changes in response characteristics during prolonged visual motion stimulation. By simultaneous recordings of synaptically coupled neurons, we were able to directly compare adaptation-induced effects at two consecutive processing stages in the fly visual motion pathway. This allowed us to narrow the potential sites of adaptation effects within the visual system and to relate them to the properties of signal transfer between neurons. Motion adaptation was accompanied by a response reduction, which was somewhat stronger in postsynaptic than in presynaptic cells. We found that the linear representation of motion velocity degrades during adaptation to a white-noise velocity-modulated stimulus. This effect is caused by an increasingly nonlinear velocity representation rather than by an increase of noise and is similarly strong in presynaptic and postsynaptic neurons. In accordance with this similarity, the dynamics and the reliability of interneuronal signal transfer remained nearly constant. Thus, adaptation is mainly based on processes located in the presynaptic neuron or in more peripheral processing stages. In contrast, changes of transfer properties at the analyzed synapse or in postsynaptic spike generation contribute little to changes in velocity coding during motion adaptation.

Key words: **dual recording; insect; motion adaptation; synapses; velocity encoding; vision**

Introduction

Neuronal adaptation is usually regarded to improve the representation of the outside world, for instance, by enhancing the efficiency of sensory coding (Brenner et al., 2000; Maravall et al., 2007). However, although many adaptation-induced changes in neuronal response properties have been described, relatively little is known about the nature and localization of the underlying physiological mechanisms (for review, see Kohn 2007).

Visual motion-sensitive neurons in the fly brain have been used as a model system for understanding how visual interneurons adapt to maintained stimulation (Maddess and Laughlin, 1985; Harris et al., 2000). These cells belong to the so-called tangential cells (TCs) in the lobula plate. TCs integrate the outputs of many local motion-sensitive elements and thus possess large receptive fields (Hausen, 1984; Egelhaaf et al., 2002; Egelhaaf, 2006). Similar to many neurons in other sensory systems, fly TCs decrease their response magnitude during sustained stimulation, along with more complex changes in response properties (Brenner et al., 2000; Fairhall et al., 2001). Time-evolved response changes have generally been called adaptation, although some of these changes result directly from the properties of the motion detection mechanism (Borst et al., 2005). These effects interact with adaptation processes that require activity-dependent changes in system parameters (Maddess and Laughlin, 1985; Harris et al., 2000). Such changes are thought to originate at both peripheral and more central processing stages, although their exact cellular localization and mechanisms are essentially unknown (Kurtz, 2007). Moreover, it has not yet been assessed to what extent the representation of different frequencies of velocity fluctuations is affected by adaptation.

Here we compared adaptation in the fly visual motion pathway at two consecutive processing stages connected by identified synapses, the VS–V1 circuit. The 10 VS ("vertical system") cells respond to vertical motion in dorsoventrally elongated sections of the visual field along different azimuth positions with graded potential changes in their axons. These graded potentials may be superimposed by spikes of variable amplitude (Hengstenberg, 1982; Krapp et al., 1998). The V1 cell receives visual motion information from the four most frontal VS cells and transforms the resulting postsynaptic potentials into spike activity (Kurtz et al., 2001). This synaptic connection provides linear and robust transfer of information from VS to V1 on fluctuations in motion velocity of up to 10 Hz (Warzecha et al., 2003; Kalb et al., 2006; Beckers et al., 2007). By simultaneous recordings of presynaptic and postsynaptic activity, we were able to narrow the potential sites of adaptation-induced effects: adaptation effects that are present in the V1 cell, but not in VS cells, arise during synaptic transfer or in the postsynaptic cell itself.

We found similar adaptation-induced changes in presynaptic VS cells and the postsynaptic V1 cell. Consequently, a direct assessment of interneuronal signal transfer showed that signaling from VS to V1 remained almost unchanged with adaptation.

Received Sept. 7, 2007; revised July 15, 2008; accepted July 16, 2008.

This work was supported by grants from the Deutsche Forschungsgemeinschaft. We thank three anonymous reviewers for their helpful comments on previous versions of this manuscript.

Correspondence should be addressed to Rafael Kurtz, Department of Neurobiology, Bielefeld University, P.O. Box 100131, D-33501 Bielefeld, Germany. E-mail: rafael.kurtz@uni-bielefeld.de.

DOI:10.1523/JNEUROSCI.1936-08.2008

 0270-6474/08/289183-11$15.00/0

Moreover, our results suggest a shift from fairly linear velocity representation in the unadapted state to increasingly nonlinear coding in the adapted state.

Materials and Methods

Preparation and electrophysiology

Female 1- to 2-d-old blowflies (*Calliphora vicina*) were obtained from our laboratory culture and dissected as described previously (Dürr and Egelhaaf, 1999) with the modification that both hemispheres of the brain instead of only one were exposed. Experiments were performed at room temperatures (20–23°C). An experiment was started by extracellularly recording the V1 cell in its output arborization in the left optic lobe. The V1 cell was identified by its sensitivity to downward motion in the frontal region of the right visual field (Krapp et al., 2001). The V1 spike activity was recorded with glass electrodes (GC150TF-10; Clark Electromedical) pulled on a GMZ Universal puller (Zeitz) with resistances of 4–8 MΩ when filled with 1 M KCL. Spikes were detected by a threshold operation, converted into pulses of fixed height, sampled at 5 kHz, and analog-to-digital converted (DT 3001; Data Translation). Once a stable V1 recording was obtained, a presynaptic VS cell was intracellularly recorded close to its output terminal in the right hemisphere of the brain. Presynaptic VS cells could be identified by graded depolarizations during presentation of downward motion in frontal regions of the right visual field (Krapp et al., 1998). The membrane potential of a recorded VS cell was analog-to-digital converted at a rate of 5 kHz. Glass electrodes for intracellular recordings were pulled on a Brown Flaming puller (P97; Sutter Instruments) and had resistances between 30 and 50 MΩ when filled with 1 M KCL.

Experimental protocol

Dynamic motion stimulation. We used vertically moving square-wave gratings as adapting stimuli (spatial wavelength, 12°; mean luminance, 15.6 cd/m^2; brightness contrast, 0.54), which were generated by a computer-controlled image synthesizer (Picasso; Innisfree) and displayed on a cathode ray tube (model 608; Tektronix) at a frame rate of 183 Hz. The center of the monitor screen was at an azimuth/elevation of −55°/26°, with 0° corresponding to the frontal midline of the blowfly. The horizontal extent of the stimulus pattern was 90°, and the vertical extent corresponded to 110°. The velocity of the moving stimulus pattern was randomly modulated. We generated two different low-pass-filtered Gaussian white-noise velocity fluctuations with a SD of 100°/s and an average velocity of 0°/s. The cutoff frequency of the low-pass filter was 80 Hz to avoid aliasing with the frame rate of the monitor. A whole adapting motion stimulus consisted of six consecutive identical motion sequences, each lasting 1.28 s.

Constant motion stimulation. Some of the experiments were performed using constant velocity motion stimulation (see Fig. 2). A detailed description of the stimuli was given by Kurtz et al. (2001). In brief, stimuli consisted of apparent-motion square-wave gratings that were generated by a light-emitting diode board. The grating had a mean luminance of 509 cd/m^2, a brightness contrast of 0.99, and a spatial wavelength of 32° and moved with a temporal frequency of 4 Hz, corresponding to a velocity of 128°/s .

Data analysis. Data were analyzed off-line using routines written in Matlab 6.5 (MathWorks).

We subtracted the baseline spike activity and the resting membrane potentials from all analyzed V1 and VS cells, respectively. To analyze the spike responses of postsynaptic V1 cells, we calculated the time-dependent instantaneous spike rate as the inverse of interspike intervals from individual spike trains.

To characterize the decline of presynaptic and postsynaptic signals through the course of adaptation, we identified the periods of time during which the stimulus pattern moved in the preferred direction and averaged over corresponding response segments (see Fig. 3). This was done because valid comparisons between VS and V1 need to account for the fact that V1 can only code preferred direction velocity attributable to the low spontaneous activity and the rectification imposed by the spike-generation process.

We characterized the gain of signal transfer between VS and V1 by subdividing the presynaptic potential into voltage classes and averaging over the corresponding postsynaptic spike responses (inverse of interspike intervals). Thus, the mean and the SD of postsynaptic spike rates were plotted as a function of the presynaptic potential (see Fig. 4*A*).

To analyze the relationship between the presynaptic or postsynaptic response and the dynamic motion stimulus, we assessed the neuronal responses elicited by the corresponding instantaneous motion velocity at each time bin. The presynaptic and postsynaptic signals were shifted according to the response latency obtained from the cross-correlation of the responses and the velocity profile of the motion stimulus. Similar to the characterization of the transfer gain, we split the motion velocities into classes and calculated the mean and the SD of presynaptic potentials and postsynaptic spike rates as a function of the motion velocity class (see Fig. 5*A*,*B*).

We used coherence analysis to evaluate the dynamic relationship between the presynaptic and the postsynaptic signals as well as between the neuronal responses of either the presynaptic or the postsynaptic neurons and the stimulus over the course of adaptation (see Figs. 4*B*,*C*, 5*C*,*D*). The coherence quantifies the frequency-dependent similarity between a given signal and a reconstructed version of the signal. For our analysis, we reconstructed the presynaptic potential from the postsynaptic spike activity, as well as the motion velocity profile of the stimuli from the neuronal responses. For all coherence calculations, the presynaptic and postsynaptic signals were shifted according to the response latency obtained from the cross-correlation of the responses and the velocity profile of the motion stimulus. The reconstruction followed well established linear filtering procedures (Gabbiani and Koch, 1998; Warzecha et al., 2003). In brief, when reconstructing a time-dependent stimulus $s(t)$ from a response $r(t)$, the reverse linear filter that minimizes the mean square error between the reconstructed stimulus and $s(t)$ is given in frequency space by the following:

$$H(f) = \langle\langle R_i^*(f) \cdot S_i(f) \rangle\rangle / \langle\langle R_i(f) \cdot R_i^*(f) \rangle\rangle. \quad (1)$$

$R_i(f)$ and $S_i(f)$ are the Fourier transforms of $s(t)$ and $r(t)$, respectively. The brackets $\langle\ \rangle$ denote averages over time segments of the stimulus (S_i) and the corresponding responses (R_i); · denotes the dot product, and * denotes the complex conjugate. The stimulus can then be reconstructed in the time domain by convolving the response $r(t)$ with the impulse response of $H(f)$ obtained by reverse Fourier transformation. To quantify to what extent the stimulus $s(t)$ is transformed linearly and reliably into the response $r(t)$, the coherence function can be calculated by the following:

$$\gamma^2(f) = \langle\langle R_i^*(f) \cdot S_i(f) \rangle\rangle \cdot \langle S_i^*(f) \cdot R_i(f) \rangle\rangle / \langle\langle S_i(f) \cdot S_i^*(f) \rangle\rangle \cdot \langle R_i(f) \cdot R_i^*(f) \rangle\rangle. \quad (2)$$

In case the coherence γ^2 equals 1 for all frequencies f, the relationship between the signals is linear and noise free, whereas a coherence below 1 is attributed to noise and/or nonlinearities in the system.

To analyze whether coherence values below 1 are caused by an increase of noise or an increase of nonlinearities (or to a combination of both effects), we determined the so-called expected coherence (see Fig. 6). The expected coherence is defined as the coherence between individual neuronal responses and the corresponding "noise-free" averaged stimulus-induced response component (Haag and Borst, 1997; van Hateren and Snippe, 2001). Whereas expected coherences below 1 indicate the presence of noise, any deviation between the coherence and the expected coherence can be attributed to nonlinearities. Expected coherence values can be overestimated with too small datasets. To exclude this possibility, we repeated the same analyses with datasets reduced to half their original size. These control analyses yielded similar results as obtained with the complete datasets and would have led to the same conclusions.

To determine the time-dependent noise, we subtracted the mean response trace from each individual response trace. We then Fourier transformed the noise traces to obtain the noise spectra (see Fig. 6).

We finally investigated the impact of adaptation on the sensitivity to acceleration of both the presynaptic and the postsynaptic neurons (see Fig. 8). Because the acceleration sensitivity may depend on the current

instantaneous motion velocity, we first divided the stimulus into velocity classes. For each velocity class, we divided the corresponding acceleration values into two equally sized classes of low and high acceleration. The mean neuronal responses for each velocity class were determined separately for the two acceleration classes. Finally, the relative attenuation of adaptation-induced acceleration sensitivity was calculated by the following formula:

$$\text{attenuation ratio} = (r\text{high}_{\text{unadapted}} - r\text{high}_{\text{adapted}})/(r\text{low}_{\text{unadapted}} - r\text{low}_{\text{adapted}}), \quad (3)$$

where *r*high is the average response elicited by high acceleration values, and *r*low is the average response elicited by low acceleration values.

Results

We performed dual recordings of synaptically coupled visual motion-sensitive neurons in the fly brain to directly compare the effects of motion adaptation on the neuronal response profiles at two successive processing stages in the fly visual system. The postsynaptic V1 cell integrates the graded output signals from at least four presynaptic VS cells, namely VS1–VS4, translates the resulting postsynaptic signals into spike activity and transmits the spikes to the contralateral brain hemisphere (Kurtz et al., 2001; Kalb et al., 2006). The synapses between the presynaptic VS cells and the postsynaptic V1 cell were shown to operate almost linearly over a wide range of presynaptic membrane potential fluctuations elicited by visual motion stimulation (Kurtz et al., 2001; Warzecha et al., 2003) or by voltage clamp of one presynaptic neuron (Beckers et al., 2007). Moreover, there is evidence that the connections between the VS cells and the V1 cell are established by a combination of chemical and electrical synapses (Haag and Borst, 2004; Kalb et al., 2006).

We identified presynaptic VS cells by their receptive field properties and tested their synaptic coupling to the V1 cell by injecting positive and negative current into VS and observing the corresponding simultaneous increases or decreases in V1 spike activity. We restricted our experimental analysis to presynaptic VS cells, which provide strong input to their postsynaptic target, namely VS1–VS3 (Kalb et al., 2006). To analyze adaptive changes in the temporal response characteristic of presynaptic and postsynaptic cells during maintained motion stimulation, we used repeated velocity-modulated motion sequences (Fig. 1). The entire adaptation protocol consisted of six consecutive identical motion sequences (see Materials and Methods). As can be seen from the section of the sample dual recording shown in Figure 1, both the presynaptic and the postsynaptic cells followed the velocity modulations during periods of downward motion, i.e., motion in the preferred direction of the cells (Fig. 1*B*). Conversely, upward motion hyperpolarized the presynaptic VS cell in a graded manner, whereas the postsynaptic V1 cell stopped spiking almost completely. Both the presynaptic and the postsynaptic motion-induced response amplitudes gradually decreased from the first to the sixth presentation of the motion sequence. This is most prominent during phases of sustained preferred direction motion, which induce sustained activity in the unadapted state but only a transient burst of activity in the adapted state (Fig. 1*B*, compare black and gray traces).

In the following, we will address whether the response reduction with motion adaptation is associated with functional consequences, in particular for the coding of velocity fluctuations by presynaptic and postsynaptic cells. Because we investigated the response properties of consecutive synaptically coupled cells in the visual pathway at the same time, we could scrutinize whether the signal transfer between these neurons contributes to motion adaptation.

All in all, our analysis is based on five cell pairs, which have been simultaneously recorded during dynamic motion adaptation. An additional set of five V1 cells, stimulated with fluctuating motion velocities, was included for the analyses shown in Figure 8. A different dataset was used for testing adaptation to constant-velocity motion ($n = 12$ VS cells; $n = 9$ V1 cells).

Impact of motion adaptation on the neuronal response magnitude during visual motion stimulation

Is response attenuation of presynaptic VS cells and the postsynaptic V1 cell similar during adaptation with a constant-velocity motion stimulus as during adaptation with fluctuating motion velocities?

Both VS and V1 cells exhibited a characteristic decline in response amplitude during the adaptation with constant-velocity motion: after a phase of continuous response reduction over a time period of ~5 s stimulation, the motion-induced response amplitudes reached a fairly constant steady-state level (Fig. 2).

The stimulus-induced responses also decreased through the course of dynamic motion adaptation (compare Fig. 1). To compare this adaptation-induced effect between the presynaptic and the postsynaptic cells, we quantified the corresponding response amplitudes elicited by each repetition of the dynamic motion sequence. To account for the rectification inherent in the spike-generation process of postsynaptic V1 cells, we restricted the analysis to time segments of preferred-direction motion (see Materials and Methods).

Figure 3 illustrates the reduction of the response amplitudes with repetition of the dynamic motion sequence and, thus, the buildup of motion adaptation. Because a single dynamic motion sequence lasted 1.28 s, the plotted course of response decrease corresponds to a time period of 7.68 s. The motion-induced response amplitudes of postsynaptic V1 cells decreased to 0.54 ± 0.08 of the initial response magnitude, whereas the adaptation-induced attenuation of presynaptic VS cells was less pronounced, reaching 0.78 ± 0.11 (mean $\pm$ SD; $n = 5$ cell pairs) of the initial value. This effect was consistent for all analyzed cell pairs. Thus, the sensitivity to visual motion was attenuated to a larger extent in postsynaptic V1 cells than in presynaptic VS cells over the course of dynamic motion adaptation. This discrepancy suggests that the adaptation-induced response attenuation is in part generated downstream of the axonal membrane potential response of VS cells, i.e., either at the VS–V1 synapses or in the V1 cell. Note that we did not find a similar discrepancy in the adaptation-induced response decline in VS and V1 cells with constant-velocity motion (the dashed lines in Fig. 3 show corresponding adaptation-induced response decreases during constant motion adaptation).

Properties of signal transfer are essentially unaffected by motion adaptation

To investigate whether dynamic motion adaptation changes the characteristics of signal transfer between individual presynaptic VS cells and their target V1 cell, we compared the transfer properties during the period of the first (referred to as the unadapted state) and the sixth repetition (referred to as the adapted state) of the dynamic motion sequence.

We assessed the gain of the signal transfer by relating the instantaneous presynaptic membrane potential (relative to resting potential) to the corresponding instantaneous postsynaptic spike rate obtained from all five cell pairs tested in this study (Fig.

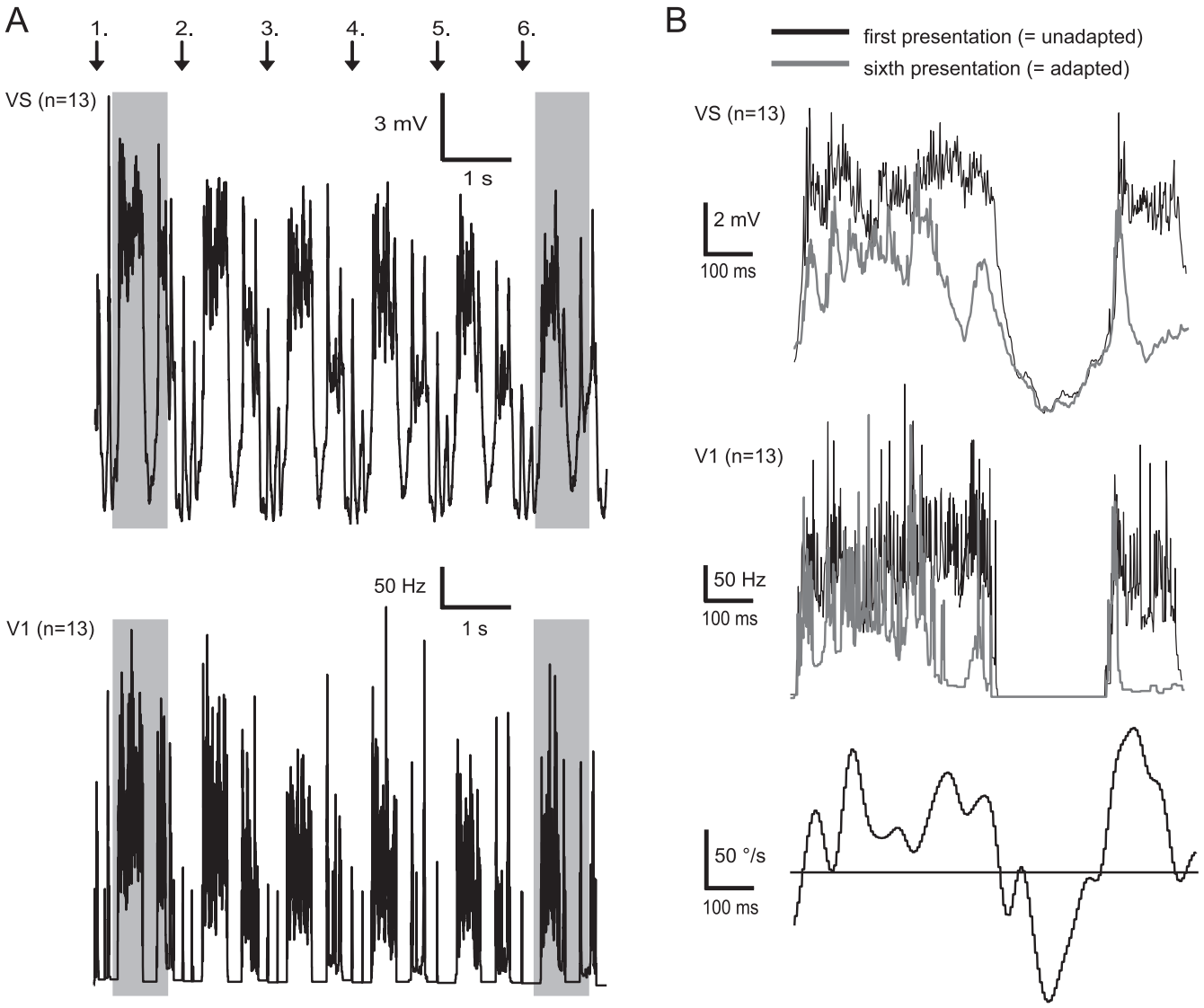

Figure 1. Adaptation of presynaptic VS cells and postsynaptic V1 cells during ongoing velocity-modulated motion. ***A***, Average response profiles of an example dual recording of a presynaptic VS cell (top) and the postsynaptic V1 cell (bottom) during motion adaptation. The cells were adapted with a motion stimulus consisting of six identical consecutive velocity-modulated motion sequences. The responses were averaged over 13 presentations of the adapting stimulus. ***B***, Section of the presynaptic and postsynaptic average responses based on the first (referred to as unadapted; black lines) and the sixth (referred to as adapted; gray lines) repetition of the single motion trials. Responses were elicited by the stimulus segment shown below. The corresponding time windows within the entire adapting motion stimulus are marked by shaded areas in ***A***.

4*A*): whereas the postsynaptic spike rate of the V1 cell did not change much when the membrane potential of the VS cell hyperpolarized during null-direction motion, it increased approximately linearly with the presynaptic depolarizations elicited by preferred-direction motion. This is in accordance with previously published results (Kurtz et al., 2001; Warzecha et al., 2003). The relationship between presynaptic and postsynaptic responses changed only insignificantly with dynamic motion adaptation. This was true, although the overall motion-induced response amplitude decreased much with adaptation and, in particular, although this response attenuation was stronger in the V1 cell than in VS cells (Fig. 3).

This poses the question why the comparatively stronger impact of dynamic motion adaptation on postsynaptic motion-induced response amplitudes is not reflected in a corresponding adaptation-induced change in transfer gain, i.e., in the slope of the postsynaptic versus presynaptic response function. The reason for this discrepancy might lay in the fact that constancy of gain between the presynaptic potential and the postsynaptic spike rate does not necessarily mean that the underlying mean activities of presynaptic and postsynaptic cells remain the same. In particular, all voltage classes across the postsynaptic versus presynaptic response function affect the slope equally but contribute differently to average activity because the number of events differs considerably between the classes (Fig. 4*A*, thin lines). Voltage classes representing fairly strong presynaptic depolarization in the range of 8–12 mV and, accordingly, leading to high postsynaptic spike rates contained a higher number of events in the unadapted than in the adapted state. In this voltage range, the transfer gain is consistently lower in the adapted state than in the unadapted state. Thus, a comparatively strong divergence between presynaptic and postsynaptic response amplitudes can exist despite only little reduction in the overall gain of signal transfer.

We also determined changes in the dynamic characteristics of signal transfer between presynaptic and postsynaptic neurons

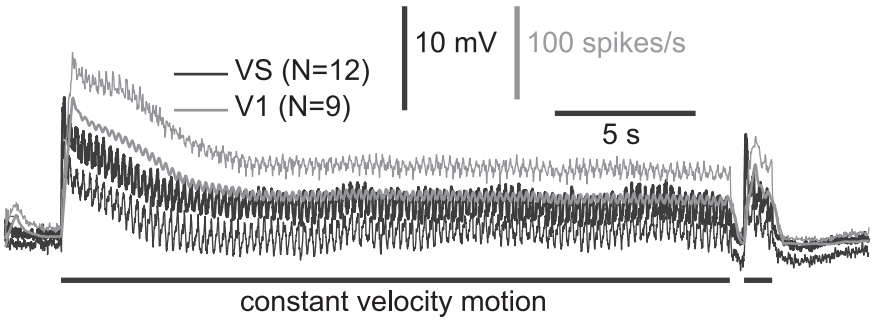

Figure 2. Adaptation of VS and V1 during ongoing constant-velocity motion. Mean responses of separately recorded 12 VS cells (thick black line; $n = 2.0 \pm 0.6$ stimulus presentations, mean $\pm$ SD) and 9 V1 cells (thick gray line; $n = 21.6 \pm 3.4$ stimulus presentations, mean $\pm$ SD) to a 24 s adapting constant-velocity motion stimulus. The thin lines show the SDs of the presynaptic (thin black line) and the postsynaptic responses (thin gray line) below and above the corresponding mean traces, respectively.

through the course of adaptation. Based on a reverse reconstruction approach, we analyzed to what extent the different frequency components of the presynaptic potential fluctuations are linearly reflected in the postsynaptic spike responses (see Materials and Methods). For this purpose, the postsynaptic spike trains were convolved with the linear filter that leads to the best estimate of the corresponding presynaptic signal. The coherence function was used to quantify the similarity between the recorded and the estimated presynaptic signal. We determined the coherence functions averaged over all trials for all analyzed cell pairs and then averaged over cells. Unadapted presynaptic potential fluctuations up to 10 Hz are, on average, transformed approximately linearly and reliably into postsynaptic spike activities, whereas the coherence value continuously decreases at higher frequencies (Fig. 4*B*, solid line). These findings are in agreement with previously published characteristics of signal transfer between single presynaptic VS cells and the postsynaptic V1 cell (Warzecha et al., 2003). In the adapted state, the signal transfer of low temporal frequency components up to 10 Hz is on average slightly reduced (Fig. 4*B*). This weak effect was similar across all analyzed cell pairs, and it developed monotonically from the first to the fifth presentation of the dynamic motion stimulus (see the course of the adaptation-induced decrease in coherences at low frequencies averaged over all analyzed cell pairs in Fig. 4*C*). We found no differences between the coherence functions obtained from unadapted and adapted responses in the higher-frequency regimen. This is reflected in the corresponding mean coherence functions shown in Figure 4*B* and was also basically the same when single cell pairs were analyzed individually. Thus, prolonged synaptic activity induced by ongoing visual motion stimulation is associated with a weak degradation of linear signal transfer in the low-frequency range up to 10 Hz.

Adaptation and the neuronal sensitivity to motion velocity

Is dynamic motion adaptation associated with a change in the velocity tuning of presynaptic and postsynaptic cells? Based on previous studies using an image step stimulation paradigm, it was suggested that local motion detectors change their temporal parameters with motion adaptation, leading to corresponding shifts in the velocity tuning of fly TCs toward higher image velocities (de Ruyter van Steveninck et al., 1986; Borst and Egelhaaf, 1987; Clifford et al., 1997) (for details, see Discussion). In accordance with Harris et al. (1999), we did not observe adaptation-induced shifts of the stimulus–response curves toward higher stimulus velocities: Figure 5, *A* and *B*, shows the average velocity tuning obtained from the unadapted (solid curves) and the adapted (dashed curves) presynaptic and postsynaptic cells. In the adapted state, both the presynaptic and the postsynaptic cells exhibited a compression of their output response ranges. The adaptation-induced compression of the output range was consistently more pronounced in postsynaptic V1 cells than in presynaptic VS cells. This discrepancy is consistent with the stronger adaptation-induced reduction of the mean response in the V1 cells than in the VS cells (Fig. 3).

Adaptation degrades linear neuronal encoding of motion velocity

Does the performance of VS and V1 to encode dynamic motion information change with motion adaptation? Again, we used coherence analysis to quantify the linear relationship between the corresponding neuronal responses and the stimulus velocity (see Materials and Methods). The coherence values obtained from presynaptic and postsynaptic neuronal responses in the unadapted state were fairly large within the frequency range of up to 10 Hz and decline with higher frequencies (Fig. 5*C*,*D*, solid lines). In accordance with Warzecha et al. (2003), the coherence functions are very similar between VS cells and the V1 cell, and the overall coherence is lower than that determined for VS–V1 transfer (compare Fig. 4*B*). However, although there is little change in the latter with adaptation, the coherences between motion stimuli and the neuronal responses decrease considerably with adaptation. This decrease comprised the entire frequency range (Fig. 5*C*,*D*, dashed lines), unlike the small decrease in coherence in VS–V1 transfer, which was limited to $<$10 Hz (Fig. 4*B*). To compare the adaptation-induced decrease in coherence between the presynaptic VS cells and the postsynaptic V1 cell, we calculated the mean coherence over the frequency range of up to 10 Hz for both the unadapted and the adapted states (Fig. 5*C*, inset): the decline in coherence was slightly more pronounced in the postsynaptic V1 cell than in the presynaptic VS cells. We observed this effect also when we analyzed single cell pairs individually. In principle, the slightly stronger decrease in coherence in the V1 cell than in VS cells might be attributable to a change in signal transfer properties or to a change in response properties of V1 cells. In particular, the spike threshold present in V1 cells could have distorted the linear representation of the stimulus velocity by V1 spike activity. A spike threshold effect might result in lower coherence values in V1 than in VS, and its impact might increase with adaptation because of the overall decrease in spike rates. The slightly stronger decrease in coherence with adaptation in the V1 cell than in VS cells (Fig. 5*C*,*D*) is thus consistent with the small difference in activity decline with adaptation between the two processing stages (Fig. 3). It is also consistent with the fact that the coherence values for the VS-to-V1 signal transfer in the low-frequency range are slightly lower in the adapted than in the unadapted state (Fig. 4*B*,*C*).

Adaptation-induced degradation of linear encoding of motion velocity is associated with an increase in nonlinear processes

A decrease in coherence with adaptation leaves open whether this change is a consequence of an increase of nonlinear processes in the transformation of a time-dependent stimulus into a neuronal response or whether an increase in noise affects the processing

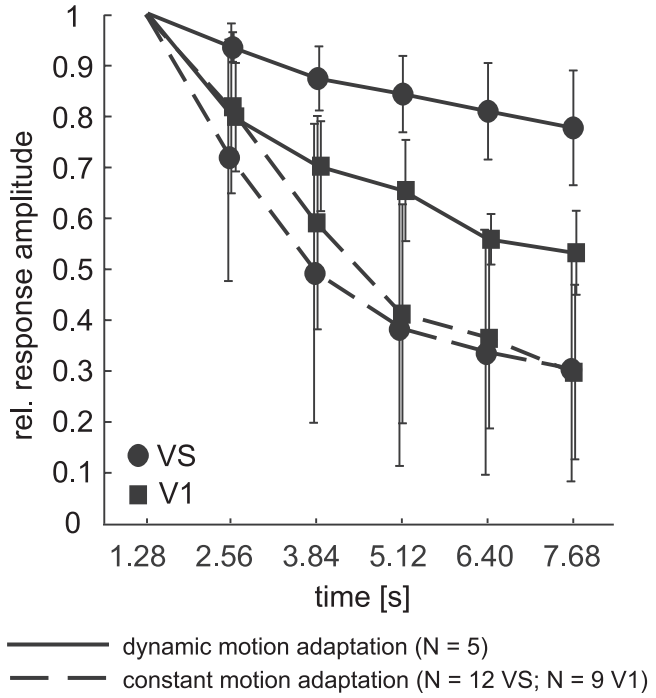

Figure 3. Time course of adaptation during presentation of constant-velocity and velocity-fluctuated motion. Relative reduction of response amplitudes of VS and V1 cells induced by adaptation with dynamic (solid lines) and constant (dashed lines) motion. To account for the rectification imposed by the spike-generation process inherent in V1 cells, the evaluation of mean responses during adaptation with dynamic motion was restricted to time periods of preferred-direction motion. For constant motion adaptation, time windows of equal size were included in the analysis. Each point in the data curves corresponds to mean responses pooled over all cells and is shown together with the respective SD. In case of dynamic motion adaptation, two different stimuli with identical statistical properties were used (see Materials and Methods). Responses were averaged over 13 consecutive presentations of each of the two dynamic adapting stimuli and then averaged over five dual VS–V1 recordings. The data based on constant motion adaptation are obtained from the responses illustrated in Figure 2. All data were normalized to the mean responses in the unadapted state. We defined the unadapted state as the time period during the first presentation of the dynamic motion sequence.

mechanisms. To disentangle these two possibilities, we determined the expected coherences for the presynaptic VS cells and the postsynaptic V1 cells based on their responses in the unadapted and in the adapted states. Because the expected coherence quantifies the similarity between individual responses and their corresponding noise-free mean response, expected coherences below 1 can be attributed to noise (see Materials and Methods). As is obvious from Figure 6, *A* and *B*, neither VS nor V1 cells exhibited a pronounced change in expected coherence as a result of prolonged stimulation with dynamic motion (compare solid and dashed lines in Fig. 6*A*,*B*). In other words, the representation of stimulus velocity by presynaptic and postsynaptic cells is not corrupted much by additional noise as a consequence of motion adaptation. Therefore, we conclude that increasingly nonlinear processing of motion in the course of adaptation leads to the decrease in coherence between the neuronal responses and the stimulus (Fig. 5*C*,*D*).

An additional approach was used to validate that the decrease in coherence associated with dynamic motion adaptation is a consequence of an increase in nonlinear processing of motion. We calculated the coherences between individual responses obtained from adapted cells and the mean responses gathered from corresponding unadapted cells. We plotted the expected coherences determined for the unadapted state as references to high-

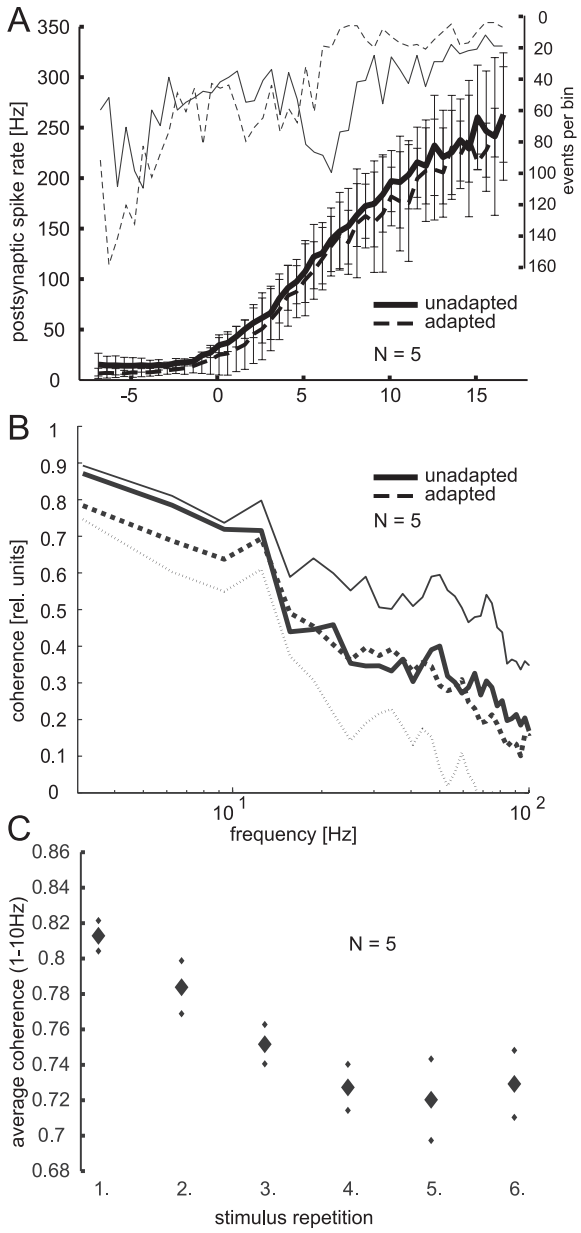

Figure 4. Impact of motion adaptation on the relationship between presynaptic and postsynaptic responses. The data analysis is based on five simultaneously recorded cell pairs. ***A***, Signal transfer gain expressed as the mean and the SD of the postsynaptic spike rate as a function of the presynaptic membrane potential obtained from unadapted (solid line) and adapted (dashed line) states. The presynaptic voltage traces were subdivided into 0.5 mV classes, and, for each instant of time, the postsynaptic spike rate was assigned to the corresponding presynaptic voltage class. The thin solid and dashed lines show the number of events per analyzed class of presynaptic voltage in the unadapted and in the adapted state, respectively (plotted on right axis; note the inverted axis orientation). Data were averaged over all five cell pairs. ***B***, The similarity between presynaptic membrane potentials and postsynaptic spike responses was quantified by the coherence analysis. The coherence values indicate to what extent the presynaptic signal can be reconstructed by convolution of the postsynaptic spike train with a linear filter. Coherence values close to 1 reflect that the corresponding frequency component of the presynaptic membrane fluctuations is linearly and reliably transformed into postsynaptic spike activities. Coherence values were averaged over all cell pairs. In the adapted state (thick dashed line), the coherences of slow frequencies of up to 10 Hz is slightly reduced compared with the unadapted (thick solid line) state. The SDs for the unadapted values (thin solid line) and the adapted values (thin dashed line) are plotted above and below the corresponding mean trace, respectively. ***C***, The mean coherence in the low-frequency range up to 10 Hz is plotted through the course of dynamic motion adaptation. Each data point denotes the mean and the SD of corresponding coherences from the first to the sixth repetition of the dynamic motion sequence. Note the difference in axis scaling between ***B*** and ***C***.

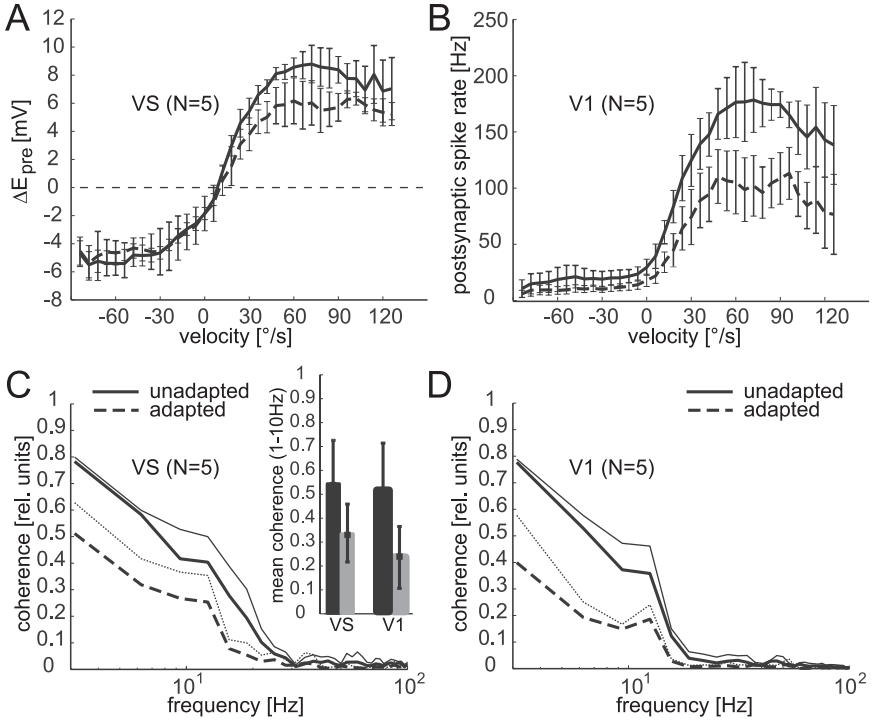

Figure 5. Stimulus representation by presynaptic VS cells and postsynaptic V1 cells. ***A***, ***B***, Velocity tuning averaged over unadapted (solid line, mean ± SD) and adapted (dashed line, mean ± SD) presynaptic and postsynaptic cells obtained from all five dual recordings. The motion sequence was subdivided into velocity classes of 6°/s, and the velocity tuning is illustrated as the mean response elicited by a certain velocity class. In accordance with the stronger response attenuation of postsynaptic V1 cells compared with VS (Fig. 3), the adaptation-induced compression of the velocity-tuning curve was also stronger in V1 cells. The dashed horizontal line in ***A*** indicates zero level to facilitate the comparison between ***A*** and ***B***. ***C***, ***D***, Representation of stimulus velocity in unadapted and adapted responses of VS and V1 cells (shown in ***C*** and ***D***, respectively) assessed by the coherence analysis. Here, the velocity of the dynamic motion stimulus was reconstructed from both unadapted (solid lines) and adapted (dashed lines) responses. Coherence values were averaged over all cells. For reasons of clarity, corresponding SDs (thin lines) are plotted only above the mean traces. The inset in ***C*** illustrates mean coherences restricted to the slow frequency range of up to 10 Hz (black bar, unadapted; gray bar, adapted). The adaptation-induced decrease of linear representation of slow-frequency fluctuations in motion velocity was more pronounced in postsynaptic V1 than in presynaptic VS cells.

light nonlinear effects arising from prolonged motion stimulation (Fig. 6*C*,*D*, averaged for all presynaptic and postsynaptic cells, respectively). Both cell types exhibited coherences of much less than 1 when determined in this way. Moreover, the similarity of the noise power spectra in the unadapted and the adapted state suggests that an increase in noise with adaptation is very unlikely (Fig. 6*E*,*F*). These findings corroborate our conclusion that dynamic motion adaptation leads to an increase in nonlinearities rather than to an increase in noise during the conversion of the stimulus into the neuronal response (Fig. 6, compare *A*,*B*). Because this effect was present in presynaptic as well as in postsynaptic cells, it must develop either in the visual pathway presynaptic to VS cells or originate from VS cells themselves. This conclusion is consistent with the only small decrease with adaptation in the coherence between VS and V1 responses (Fig. 4*B*).

Relationship between spike rate reduction and changes in velocity encoding with motion adaptation

It has been shown previously that, under certain stimulus conditions, the information rate of fly motion-sensitive neurons increases with increasing mean firing rate (Borst and Haag, 2001). We found a strong reduction in activity of both the presynaptic and the postsynaptic neurons with adaptation (Fig. 3). Therefore, we asked whether the increase in nonlinear representation of motion velocity and the resulting decrease in coherence between the stimulus and the neuronal response (Fig. 5*C*,*D*) is a direct consequence of the reduction in activity. We tested this by manipulating the spike responses of the V1 cell recorded in the unadapted state. Spikes were deleted by a random selection process to reduce spike rate to a distinct level. The corresponding stimulus encoding was assessed by coherence analysis. If the decrease in activity with adaptation were the consequence of a nonspecific reduction of spiking frequency, the coherence analyses would lead to similar results for datasets with similar spike rate, regardless of whether recorded from adapted neurons or obtained by manipulating the spike frequency of unadapted neurons.

The coherence obtained when reconstructing motion velocity from unadapted V1 spike trains with artificially reduced spike rates gradually decreased with decreasing overall spike rates (Fig. 7*A*). Artificial reduction of spike rate to half its original value, which is similar to the spike rate after adaptation (compare Fig. 3), did not lead to coherence values as low as those obtained for adapted V1 responses (Fig. 7*B*). This finding suggests that adaptation has a more pronounced effect on linear stimulus encoding than a pure nonspecific reduction in spike rate. More importantly, adaptation and random deletion of spikes differ qualitatively in their effect on expected coherence. Whereas the expected coherence is similar for unadapted and adapted responses (Fig. 6*B*), indicating that the decrease in coherence with adaptation is not caused by increasing noise, the expected coherence decreases after random deletion of spikes (Fig. 7*C*). Hence, random deletion of spikes manifests itself as an increase in noise, whereas a similar reduction of activity with adaptation reflects a more specific effect, namely an increase in nonlinear processing of the stimulus.

Impact of adaptation on acceleration sensitivity

The fact that the relationship between stimulus and response became more nonlinear with motion adaptation reflects a nonlinear change in velocity coding during motion adaptation. We therefore aimed to identify what kind of stimulus feature might become nonlinearly represented by the neuronal responses as a consequence of adaptation. Motivated by the previous finding that fly visual motion-sensitive cells become more sensitive to changes in image velocity during prolonged stimulation with high image velocities (Maddess and Laughlin, 1985), we tested whether motion adaptation changed the neuronal representation of stimulus acceleration in the VS and V1 cells. To do so, we calculated the adaptation-induced mean response decrease separately for segments of large and small accelerations in the adapting motion stimulus (for details, see Materials and Methods). This classification was made separately in different velocity classes to account for the inhomogeneous presence of large and small absolute accelerations in different velocity regimens. The mean response decrease at high accelerations was compared with

that at low accelerations by forming a ratio. Ratios below 1 indicate that the adaptation-induced decrease of responses at high accelerations is less pronounced than the decrease at low accelerations. Figure 8 illustrates the ratios indicating the relative attenuation of the neuronal response at high versus low accelerations for the different velocity classes. Values of 1 (marked by the dashed line) indicate that there is no difference in the decrease of response with adaptation at high and low accelerations. Overall, a larger proportion of ratio values is smaller than 1, indicating that the neuronal sensitivity was slightly less attenuated at high than at low accelerations (Fig. 8). This effect was more pronounced in V1 cells (72% of the ratios are below 1; median value, 0.79) (Fig. 8*B*) than in VS cells (60.6% of the ratios are below 1; median value, 0.69) (Fig. 8*A*) and reached significance (one-sided sign test, $p < 0.05$) in some of the velocity classes for V1 cells (Fig. 8*B*, asterisks) but in none of the classes for VS cells.

Altogether, adaptation leads to a strong reduction in response amplitude together with a profound decrease in the linear representation of stimulus velocity. However, because of nonlinear features of the adaptation process, the sensitivity to high accelerations, i.e., fast changes in the velocity-modulated stimulus, appears to be represented more strongly than slow changes. These changes are similar in VS and V1, indicating that signal transfer between these neurons is not much affected by adaptation.

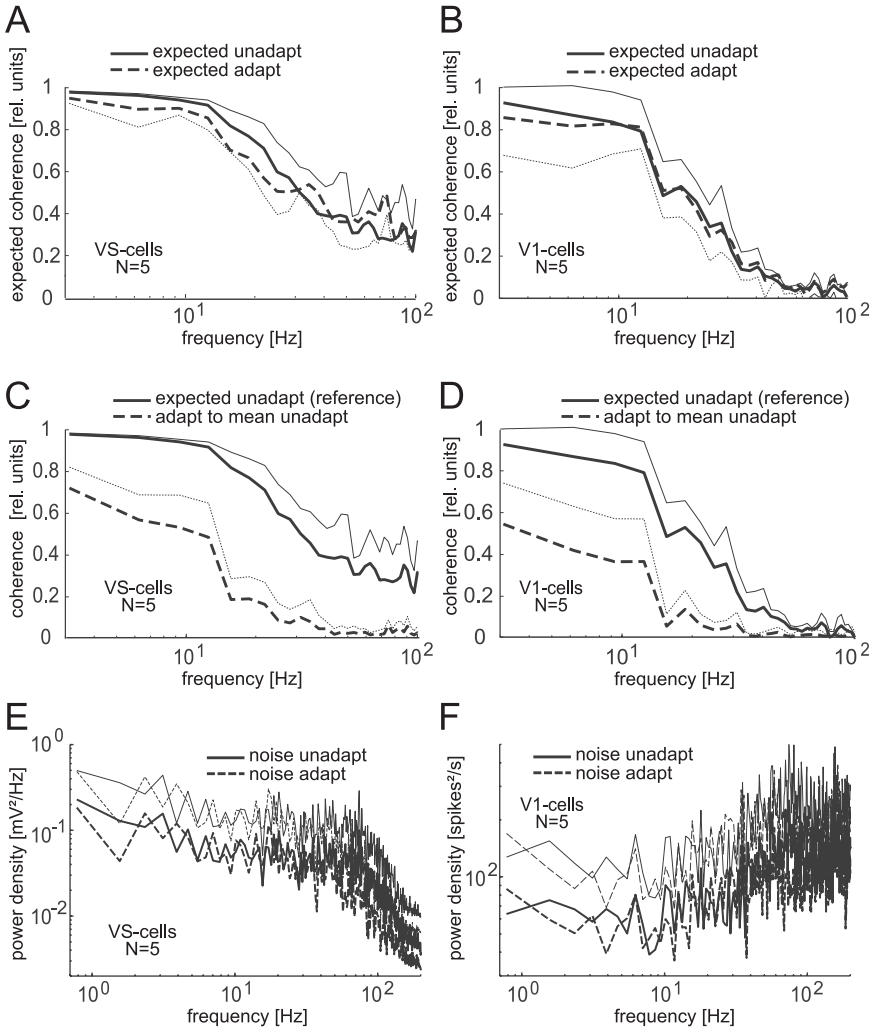

Figure 6. Contribution of noise to adaptation-induced changes in stimulus representation. ***A***, ***B***, The mean expected coherence of presynaptic (***A***) and postsynaptic (***B***) cells was quantified as the coherence between individual neuronal responses and their corresponding noise-free averaged stimulus-induced response component. Expected coherences did not change as a result of dynamic motion adaptation (compare solid with dashed curves). Thus, motion adaptation did not increase the noise in the system. Corresponding SDs (thin lines) are plotted in opposite directions. ***C***, ***D***, The coherence between single adapted responses and the corresponding mean response in the unadapted state (dashed lines) is shown (***C***, VS cells; ***D***, V1 cells). For comparison, the expected coherence in the unadapted state is redrawn (solid lines, identical to those shown in ***A***, ***D***). Because adaptation did not increase the noise, the reduction in coherence values can be attributed to an increase in nonlinearities. ***E***, ***F***, The mean noise spectra for the unadapted state (solid lines) and the adapted state (dashed lines) are shown (***E***, VS cells; ***F***, V1 cells; SDs shown above the mean traces by the corresponding thin lines).

Discussion

We analyzed the impact of motion adaptation on the response properties of synaptically coupled motion-sensitive neurons within an identified motion-processing circuit in the fly visual system. The impact of adaptation was found to be similar in presynaptic VS cells and their target V1 cell. Accordingly, the gain and the dynamic characteristics of signal transfer from VS cells to the V1 cell changed only little during ongoing presynaptic activity. The ability to linearly encode stimulus velocity degrades with adaptation in the presynaptic VS cells as well as in their target V1 cell. This degradation is concluded to be mainly caused by an increase in nonlinearities in the neuronal representation of stimulus velocity during dynamic motion adaptation.

Localization of the adaptational processes

Motion adaptation induced a profound decrease in response magnitude in presynaptic VS cells as well as in the postsynaptic V1 cell (Figs. 1–3). Hence, adaptation is to a large extent generated upstream of the V1 cell. In analogy, it was concluded that contrast gain control over the receptive field center of mammalian retinal ganglion cells originates primarily from changes at the level of synaptic input rather than from changes in ganglion cells themselves (Manookin and Demb, 2006). During dynamic motion adaptation, the response reduction in the postsynaptic V1 cells was somewhat stronger than that in the presynaptic VS cells, corroborating results from a voltage-clamp study: here the postsynaptic spike rate decreased slightly over time when the presynaptic voltage was held at a depolarized level (Beckers et al., 2007). The stronger response attenuation in the V1 cell than in VS cells with adaptation might be attributable to changes in the properties of VS–V1 synapses or changes within the postsynaptic V1 cell itself. Constant velocity motion did not lead to a similar discrepancy in response adaptation between presynaptic and postsynaptic cells (Fig. 3). As a possible explanation for this difference, constant velocity motion elicits stronger adaptation in the peripheral visual system and in VS cells than the dynamic motion stimulus, because a sustained depolarization is induced.

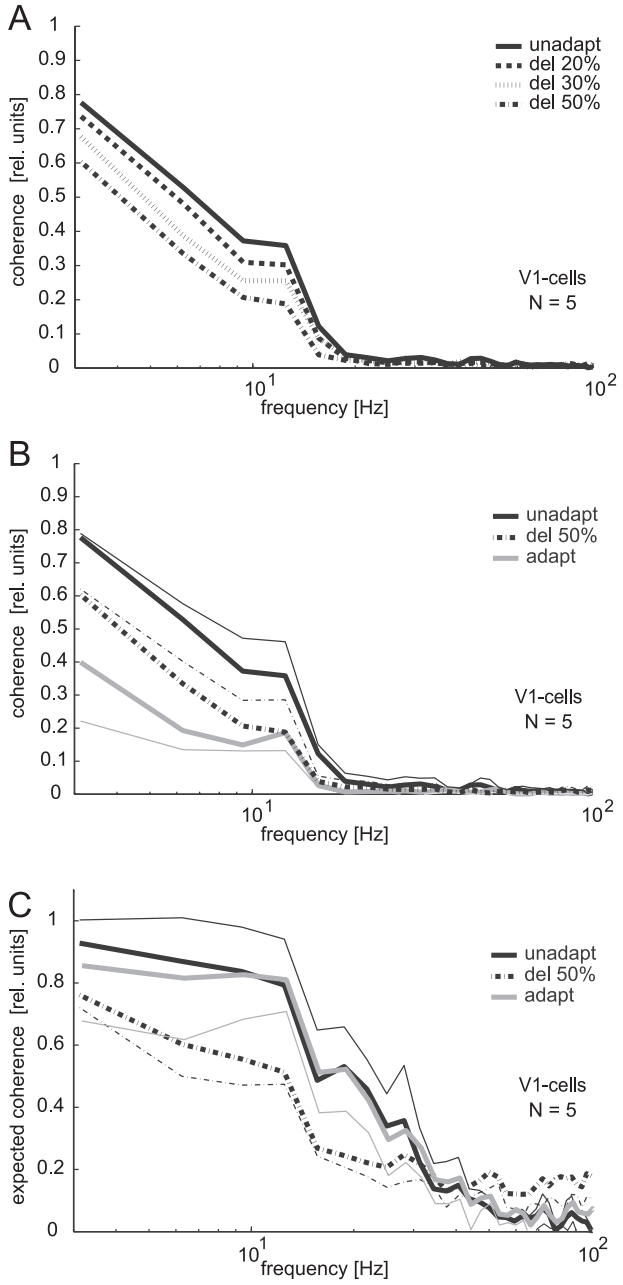

Figure 7. Influence of spike rate on velocity encoding. ***A***, To test whether a reduction of spike rate affects the linear representation of motion velocity, 20, 30, or 50% of the spikes were randomly deleted from the spike trains recorded from five V1 cells (same cells as in Figs. 4–6) in the unadapted state during presentation of velocity fluctuations. Artificial spike rate reduction led to a decrease in the mean coherence functions (different dashed and dotted lines) relative to the original traces from the unadapted cells (solid line, replotted from Fig. 5*D*). ***B***, Coherence for the V1 cells in the unadapted state (solid black line, replotted from ***A***, with SD plotted above) and the adapted state (gray line with SD plotted below, replotted from Fig. 5*D*) and for the manipulated dataset obtained by randomly deleting 50% of the spikes from unadapted spike trains (dashed line with SD plotted above), thus reaching a similar activity level as after adaptation. ***C***, Expected coherence in the unadapted state (solid black line with SD plotted above, replotted from Fig. 6*B*) and for the dataset manipulated to reach a 50% reduction in spike rate (dashed line, with SD plotted below). Unlike adaptation the artificial reduction in spike rate led to a decline in the coherence (compare the dashed line with the gray line, replotted from Fig. 6*B*).

Note also that, during constant velocity adaptation, pattern luminance was higher than during dynamic motion adaptation. Thus, when adapted to constant motion, the low presynaptic activity might avoid additional activity-dependent adaptation at synapses between VS cells and V1 and/or adaptation in the postsynaptic V1 cell itself. In contrast, during dynamic motion stimulation, VS cell activity adapts less and might, from time to time, reach depolarization levels that are high enough to induce additional adaptational processes downstream of VS cells.

In addition to the response attenuation, the linear encoding of motion velocity was profoundly degraded with adaptation. This degradation is, if at all, only slightly more pronounced in V1 cells than in VS cells (Fig. 5*C*,*D*), corroborating that VS-to-V1 signal transfer does not change much during adaptation. Hence, the adaptational processes that change velocity coding are located within VS cells and/or at peripheral motion processing stages of the visual system.

Mechanisms underlying the observed changes in response properties

Although several changes in response properties of fly TCs with ongoing visual motion stimulation have been described (Maddess and Laughlin, 1985; Brenner et al., 2000; Harris et al., 2000; Borst et al., 2005), comparatively little is known about the underlying cellular mechanisms of motion adaptation. A fast alignment of the input–output gain of TCs with the SD of velocity fluctuations can be attributed to inherent properties of correlation-based motion detectors, which are thought to form the computational principle of fly motion detection (Borst et al., 2005). Because these inherent processes evolve very fast after a change in stimulus parameters, they will probably not contribute much to the rather slow adaptation phenomena observed with our stimulation paradigm (Figs. 1, 3).

A direction-selective component of motion adaptation emerges in fly TCs from the activity-dependent increase of an inhibitory conductance and results in an afterhyperpolarization (Kurtz, 2007), similar to visual cortical neurons (Carandini and Ferster, 1997). As a consequence, the stimulus–response functions of TCs are shifted downward (Harris et al., 2000; Kurtz et al., 2000). Harris et al. (2000) identified two additional adaptation components that are insensitive to motion direction. All three components were found to reduce the contrast gain of fly TCs and are likely to contribute to the changes in response properties observed in our study. In particular, the compression of the velocity-response functions with adaptation (Fig. 5*A*,*B*) might be attributable to a contrast gain reduction, because lowered contrast sensitivity will lead to a decline in the responses to stimuli with fixed contrast.

In accordance with Harris et al. (1999), we did not observe adaptation-induced shifts of the velocity-response functions toward higher motion velocities (Fig. 5*A*,*B*). Such shifts were predicted, because the responses of TCs to brief image displacements (so-called impulse responses) decayed faster in the adapted than in the unadapted state, hinting at a shortening of delay filters in correlation-based motion-detector circuits (de Ruyter van Steveninck et al., 1986; Clifford et al., 1997). The increased transience of responses to velocity modulations with motion adaptation (Fig. 1) is reminiscent of the change of the impulse responses (de Ruyter van Steveninck et al., 1986). These changes might be the result of a shortening of a high-pass filter, rather than of the delay filter, in the motion-detector, as is suggested by modeling studies (Borst et al., 2003; Safran et al., 2007).

The major adaptation effect induced by our stimulus paradigm was a decrease in the coherence between motion velocity and the corresponding neuronal responses (Fig. 5*C*,*D*). Rather than being the result of increased noise, this effect is attributable to an increasingly nonlinear relationship between velocity and

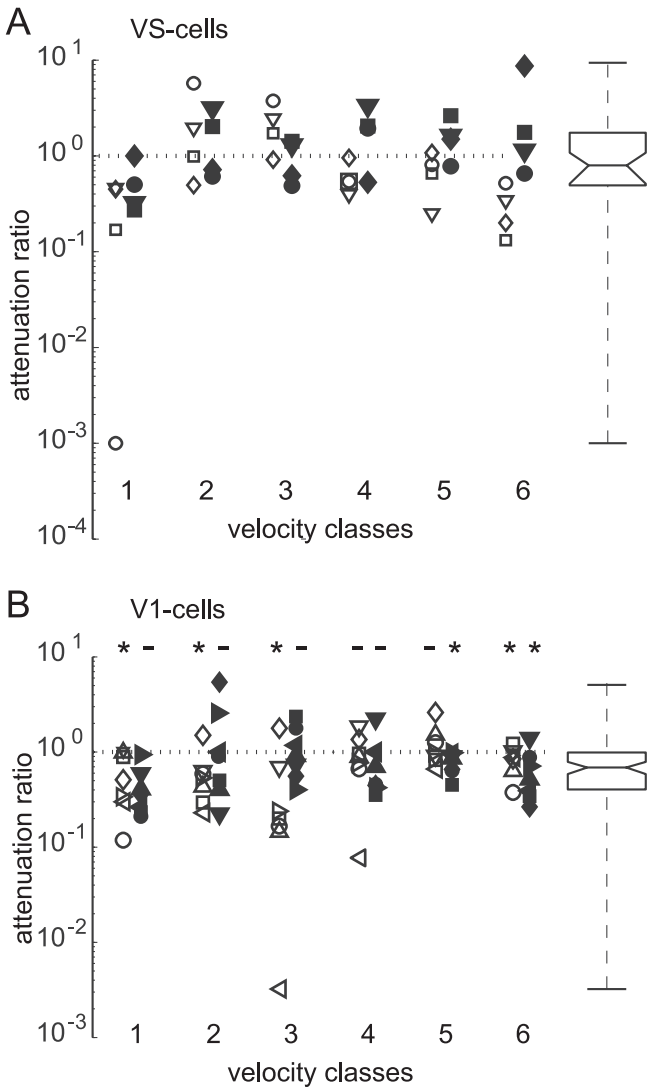

Figure 8. Impact of adaptation on sensitivity to acceleration. For the analysis, the stimulus was divided into six velocity classes, each covering a range of 10°/s. The lowest velocity class ranged from 0 to 10°/s, and the highest velocity class ranged from 50 to 60°/s. For each velocity class, the acceleration values were divided into two equally sized groups of high or low accelerations. The relative neuronal sensitivity of VS and V1 cells (shown in ***A*** and ***B***, respectively) to stimulus acceleration was assessed by the ratio of the adaptation-induced decrease of responses elicited by high accelerations to the decrease of responses elicited by low accelerations (see Materials and Methods). A ratio of 1 (indicated by the dashed line) indicates that there is no difference between adaptation-induced response attenuation at high and low accelerations. Ratios below 1 reveal a stronger response reduction at low acceleration compared with the attenuation at high acceleration. Two different dynamic adapting stimuli with identical statistical properties were used (see Materials and Methods). The results obtained with the two stimuli were analyzed separately, illustrated as open and filled data symbols. For the evaluation, data of additional five V1 neurons that were not recorded together with VS neurons were included. Different symbols denote data from different cells. In ***B***, asterisks mark columns of data that are significantly smaller than 1, whereas nonsignificant data columns are marked by a dash (one-sided sign test, $p < 0.05$). Box whisker plots show the distribution of the ratios: the horizontal lines of the boxes indicate the upper quartile, median, and lower quartile values. Whiskers show the extent of the rest of the data.

neuronal response in the course of adaptation (Fig. 6). This conclusion is corroborated by a study using naturalistic optic flow as motion stimulus and assessing changes in the linear relationship between unadapted and adapted responses (Heitwerth et al., 2005). This study reported a slightly smaller adaptation-induced increase in nonlinearities than has been inferred from our experiments. This discrepancy might be attributable to the fact that the analysis was based on another TC than our study and that the statistical properties of naturalistic stimuli differ from those of the white-noise velocity fluctuations.

Nonlinear effects of adaptation have also been reported in other sensory systems. For instance, adaptation was found to induce a nonlinear change in the frequency encoding of sensory interneurons in the cercal sensory system of crickets (Clague et al., 1997). Here, the identified nonlinearity was associated with a disproportionate loss of information about high-frequency stimulus components. This was different in the present study: low frequencies appear to be more affected by adaptation than high frequencies (Figs. 4*B*,*C*, 8). A relative loss of power at low frequencies was also demonstrated in a modeling study of adaptation in visual cortical neurons and was interpreted as being useful in the context of redundancy reduction (Wang et al., 2003).

Functional relevance of the adaptation-induced changes in response properties

We found evidence of an increase in nonlinearities in the velocity–response relationship induced by motion adaptation (Fig. 6*C*,*D*). Changes between linear and nonlinear velocity–response relationship depending on adaptational state increase ambiguities in velocity coding but may help the system to reduce overall activity during sustained stimulation but remain sensitive to fast changes in stimulus velocity (Fig. 8). The decrease in response amplitude might in itself be beneficial given the metabolic costs of neuronal activity (Laughlin, 2001; Kohn, 2007). In accordance with our study, Maddess and Laughlin (1985) found an increase in relative sensitivity of the fly H1 neuron to changes in the motion velocity, whereas the steady-state responses decrease with motion adaptation, indicating that it is not the prime function of TCs to represent motion velocity veridically. In flight situations, this adaptational property might help TCs to respond to the presence of obstacles in the flight path, which induce strong spatiotemporal discontinuities in the optic flow (P. Liang, R. Kern, and M. Egelhaaf, unpublished observations).

Our results demonstrate a remarkable stability of transfer properties between VS and V1 cells. The reason for this stability during sustained stimulation may be that the transfer between VS and V1 is mediated by both electrical and chemical synapses, as suggested by Kalb et al. (2006). Despite an overall decrease in activity, linear and reliable signal transmission is maintained, and only a slight decline of coherences in the low-frequency regimen during ongoing synaptic activity is observed (Fig. 4*B*). Because the postsynaptic V1 cell is a heterolateral element, this property might facilitate the ability to compare motion signals from both brain hemispheres. If motion adaptation had a strong impact on synaptic transmission, such a comparison could be hampered because signals from the ipsilateral brain hemisphere pass a smaller number of synapses than the signals from the contralateral hemisphere.

References

Beckers U, Egelhaaf M, Kurtz R (2007) Synapses in the fly motion-vision pathway: evidence for a broad range of signal amplitudes and dynamics. J Neurophysiol 97:2032–2041.

Borst A, Egelhaaf M (1987) Temporal modulation of luminance adapts time constant of fly movement detectors. Biol Cybern 56:209–215.

Borst A, Haag J (2001) Effects of mean firing on neural information rate. J Comput Neurosci 10:213–221.

Borst A, Reisenman C, Haag J (2003) Adapation of response transients in fly motion vision. II. Model studies. Vision Res 43:1311–1324.

Borst A, Flanagin VL, Sompolinsky H (2005) Adaptation without parame-

ter change: dynamic gain control in motion detection. Proc Natl Acad Sci U S A 102:6172–6176.
Brenner N, Bialek W, de Ruyter van Steveninck RR (2000) Adaptive rescaling rescaling maximizes information transmission. Neuron 26:695–702.
Carandini M, Ferster D (1997) A tonic hyperpolarization underlying contrast adaptation in cat visual cortex. Science 276:949–952.
Clague H, Theunissen F, Miller JP (1997) Effects of adaptation on neural coding by primary sensory interneurons in the cricket cercal system. J Neurophysiol 77:207–220.
Clifford CW, Ibbotson MR, Langley K (1997) An adaptive Reichardt detector model of motion adaptation in insects and mammals. Vis Neurosci 14:741–749.
de Ruyter van Steveninck RR, Zaagman WH, Mastebrock HAK (1986) Adaptation of transient responses of a movement-sensitive neuron in the visual system of the blowfly *Calliphora erythrocephala.* Biol Cybern 54:223–236.
Dürr V, Egelhaaf M (1999) In vivo calcium accumulation in presynaptic and postsynaptic dendrites of visual interneurons. J Neurophysiol 82:3327–3338.
Egelhaaf M (2006) The neuronal computation of visual motion information. In: Invertebrate vision (Warrant E, Nilsson DE, eds), pp 399–461. Cambridge, UK: Cambridge UP.
Egelhaaf M, Kern R, Krapp HG, Kretzberg J, Kurtz R, Warzecha AK (2002) Neural encoding of behaviourally relevant visual-motion information in the fly. Trends Neurosci 25:96–102.
Fairhall AL, Lewen GD, Bialek W, de Ruyter Van Steveninck RR (2001) Efficiency and ambiguity in an adaptive neural code. Nature 412:787–792.
Gabbiani F, Koch C (1998) Principles of spike train analysis. In: Methods in neuronal modelling: from ions to networks, Ed 2 (Koch C, Segev I, eds), pp 313–360. Cambridge, MA: MIT.
Haag J, Borst A (1997) Encoding of visual motion information and reliability in spiking and graded potential neurons. J Neurosci 17:4809–4819.
Haag J, Borst A (2004) Neural mechanisms underlying complex receptive field properties of motion-sensitive interneurons. Nat Neurosci 7:628–634.
Harris RA, O'Carroll DC, Laughlin SB (1999) Adaptation and the temporal delay filter of fly motion detectors. Vision Res 39:2603–2613.
Harris RA, O'Carroll DC, Laughlin SB (2000) Contrast gain reduction in fly motion adaptation. Neuron 28:595–606.
Hausen K (1984) The lobula-complex of the fly: structure, function and significance in visual behaviour. In: Photoreception and vision in invertebrates (Ali MA, ed), pp 523–555. New York: Plenum.
Heitwerth J, Kern R, van Hateren JH, Egelhaaf M (2005) Motion adaptation leads to parsimonious endcoding of natural optic flow by blowfly motion vision system. J Neurophysiol 94:1761–1769.
Hengstenberg R (1982) Common visual response properties of giant vertical cells in the lobula plate of the blowfly *Calliphora.* J Comp Physiol A Neuroethol Sens Neural Behav Physiol 149:179–193.
Kalb J, Egelhaaf M, Kurtz R (2006) Robust integration of motion information in the fly visual system revealed by single-cell photoablation. J Neurosci 26:7898–7906.
Kohn A (2007) Visual adaptation: physiology, mechanisms, and functional benefits. J Neurophysiol 97:3155–3164.
Krapp HG, Hengstenberg B, Hengstenberg R (1998) Dendritic structure and receptive-field organization of optic flow processing interneurons in the fly. J Neurophysiol 79:1902–1917.
Krapp HG, Hengstenberg R, Egelhaaf M (2001) Binocular contributions to optic flow processing in the fly visual system. J Neurophysiol 85:724–734.
Kurtz R (2007) Direction-selective adaptation in fly visual motion-sensitive neurons is generated by an intrinsic conductance-based mechanism. Neuroscience 146:573–583.
Kurtz R, Dürr V, Egelhaaf M (2000) Dendritic calcium accumulation associated with direction-selective adaptation in visual motion-sensitive neurons in vivo. J Neurophysiol 84:1914–1923.
Kurtz R, Warzecha AK, Egelhaaf M (2001) Transfer of visual motion information via graded synapses operates linearly in the natural activity range. J Neurosci 21:6957–6966.
Laughlin SB (2001) Energy as a constraint on the coding and processing of sensory information. Curr Opin Neurobiol 11:475–480.
Maddess T, Laughlin SB (1985) Adaptation of the motion-sensitive neuron H1 is generated locally and governed by contrast frequency. Proc R Soc Lond B Biol Sci 228:251–275.
Manookin MB, Demb JB (2006) Presynaptic mechanism for slow contrast adaptation in mammalian retinal ganglion cells. Neuron 50:453–464.
Maravall M, Petersen RS, Fairhall AL, Arabzadeh E, Diamond ME (2007) Shifts in coding properties and maintenance of information transmission during adaptation in barrel cortex. PLoS Biol 5:e19.
Safran MN, Flanagin VL, Borst A, Sompolinsky H (2007) Adaptation and information transmission in fly motion detection. J Neurophysiol 98:339–3320.
van Hateren JH, Snippe HP (2001) Information theoretical evaluation of parametric models of gain control in blowfly photoreceptor cells. Vision Res 41:1851–1865.
Warzecha AK, Kurtz R, Egelhaaf M (2003) Synaptic transfer of dynamic motion information between identified neurons in the visual system of the blowfly. Neuroscience 119:1103–1112.
Wang XJ, Liu Y, Sanchez-Vives MV, McCormick DA (2003) Adaptation and temporal decorrelation by single neurons in the primate visual cortex. J Neurophysiol 89:3279–3293.